The Journal of Immunology
RESEARCH ARTICLE | NOVEMBER 15 2007

Involvement of Vitronectin in Lipopolysaccaride-Induced Acute Lung Injury[1]

FREE

Yuko Tsuruta; ... et. al

J Immunol (2007) 179 (10): 7079–7086.
https://doi.org/10.4049/jimmunol.179.10.7079

Involvement of Vitronectin in Lipopolysaccaride-Induced Acute Lung Injury[1]

Yuko Tsuruta,* Young-Jun Park,* Gene P. Siegal,†‡§ Gang Liu,* and Edward Abraham[2]*

Vitronectin is present in large concentrations in serum and participates in regulation of humoral responses, including coagulation, fibrinolysis, and complement activation. Because alterations in coagulation and fibrinolysis are common in acute lung injury, we examined the role of vitronectin in LPS-induced pulmonary inflammation. Vitronectin concentrations were significantly increased in the lungs after LPS administration. Neutrophil numbers and proinflammatory cytokine levels, including IL-1β, MIP-2, KC, and IL-6, were significantly reduced in bronchoalveolar lavage fluid from vitronectin-deficient (vitronectin$^{-/-}$) mice, as compared with vitronectin$^{+/+}$ mice, after LPS exposure. Similarly, LPS induced increases in lung edema, myeloperoxidase-concentrations, and pulmonary proinflammatory cytokine concentrations were significantly lower in vitronectin$^{-/-}$ mice. Vitronectin$^{-/-}$ neutrophils demonstrated decreased KC-induced chemotaxis as compared with neutrophils from vitronectin$^{+/+}$ mice, and incubation of vitronectin$^{+/+}$ neutrophils with vitronectin was associated with increased chemotaxis. Vitronectin$^{-/-}$ neutrophils consistently produced more TNF-α, MIP-2, and IL-1β after LPS exposure than did vitronectin$^{+/+}$ neutrophils and also showed greater degradation of IκB-α and increased LPS-induced nuclear accumulation of NF-κB compared with vitronectin$^{+/+}$ neutrophils. These findings provide a novel vitronectin-dependent mechanism contributing to the development of acute lung injury. ***The Journal of Immunology,*** **2007, 179: 7079–7086.**

Acute lung injury (ALI)[3] is a frequent cause of respiratory failure, affecting >200,000 patients per year in the United States (1). ALI is characterized by the infiltration of large numbers of neutrophils into the lungs, interstitial edema, fibrin leakage into the alveoli, and increased pulmonary levels of cytokines, chemokines, and other proinflammatory mediators (2–4). Neutrophils appear to play a major role in the development of ALI. Although ALI can occur in the setting of neutropenia, in both experimental models and in patients, neutrophils have been demonstrated to potentiate the pulmonary inflammatory response associated with ALI (4, 5). Given the important role that neutrophils play in ALI, central questions in the pathophysiology of this entity relate to mechanisms that contribute to the accumulation and activation of neutrophils in the lung.

Alterations in coagulation and fibrinolysis, both in the lungs and systemically, are common in the setting of ALI (6). Increased pulmonary levels of urokinase plasminogen activator (uPA) and plasminogen activator inhibitor 1 (PAI-1) are present in ALI, and both uPA and PAI-1 are able to potentiate neutrophil activation (6–10). Interaction of PAI-1 with the serine protease domain of uPA results in inhibition of the fibrinolytic, but not the proinflammatory activity of uPA, and appears to contribute to the development of microvascular thrombi and alveoli fibrin deposition that are characteristic histologic findings in ALI (6, 7, 10). Increased bronchoalveolar lavage levels of PAI-1 are associated with worse clinical outcome from ALI (11). uPA also appears to be involved in the development of ALI, since uPA-deficient mice are protected from LPS-induced pulmonary injury and Abs specific for the uPA kringle domain are protective in this setting (9, 12). The potentiating effects of uPA on LPS-induced neutrophil activation occurs through a mechanism that involves $\alpha_v\beta_3$ integrins (13). Although there is little evidence that uPA binds directly with integrins, interactions between uPA and $\alpha_v\beta_3$ integrins can occur through association of uPA with PAI-1, which generally circulates bound to the glycoprotein vitronectin (14, 15).

Vitronectin is present in large concentrations in serum, in the extracellular matrix, in platelets, and within various tissues of the human body (16–19). Circulating at micromolar levels, vitronectin participates in the regulation of humoral responses, such as coagulation, fibrinolysis, and activation of the complement cascade (16–19). Other functions of the protein include participation in cell adhesion, cell migration, and regulation of pericellular proteolysis (16–19). Vitronectin is a ligand for integrins, including $\alpha_v\beta_3$, and also promotes neutrophil adhesion and migration in vitro, at least in part through interaction with the neutrophil integrin Mac-1 ($\alpha_M\beta_2$, CD11b/CD18) as well as other receptors, such as the urokinase plasminogen activator receptor (uPAR) (14, 15, 20).

Immunohistochemical studies have shown increased expression of integrin $\alpha_v\beta_3$ and vitronectin in the inflamed lungs of sepsis patients (21, 22). However, there is little information available on the role of vitronectin in modulating neutrophil accumulation or activation during acute inflammatory processes. We therefore sought to explore the potential role of vitronectin in ALI. In this study, we demonstrate that vitronectin-deficient mice are protected from LPS-induced ALI. These findings provide a novel vitronectin-dependent mechanism contributing to neutrophil accumulation in the lungs and pulmonary injury in ALI.

*Department of Medicine, †Department of Pathology, ‡Department of Cell Biology, and §Department of Surgery, University of Alabama at Birmingham, Birmingham, AL 35294

Received for publication June 8, 2007. Accepted for publication September 6, 2007.

The costs of publication of this article were defrayed in part by the payment of page charges. This article must therefore be hereby marked *advertisement* in accordance with 18 U.S.C. Section 1734 solely to indicate this fact.

[1] This work was supported, in part, by National Institutes of Health Grants GM049222, HL062221, HL076206 (to E.A.), and AR04631 (to G.P.S.).

[2] Address correspondence and reprint requests to Dr. Edward Abraham, Department of Medicine, University of Alabama at Birmingham, Boshell Diabetes Building 420, 1530 3rd Avenue South, Birmingham, AL 35294-0012. E-mail address: eabraham@UAB.edu

[3] Abbreviations used in this paper: ALI, acute lung injury; uPA, urokinase plasminogen activator; PAI-1, plasminogen activator inhibitor 1; uPAR, urokinase plasminogen activator receptor; BAL, bronchoalveolar lavage; MPO, myeloperoxidase; MIC, Migration and Invasion Chemotaxis.

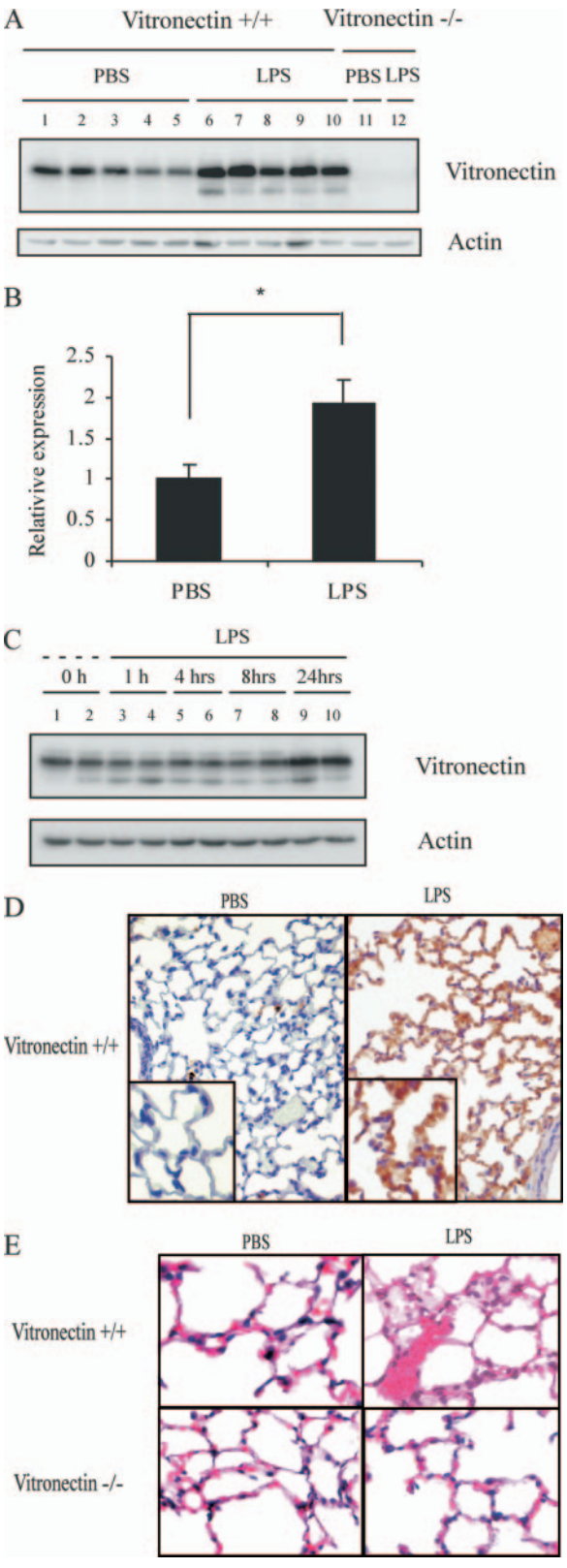

FIGURE 1. Vitronectin expression is increased in the lungs after intratracheal LPS administration. *A*, Western blotting for vitronectin in the lungs. Lungs were obtained from vitronectin$^{+/+}$ or vitronectin$^{-/-}$ mice 24 h after LPS or PBS administration. Anti-mouse vitronectin IgG was used to detect vitronectin expression in the lung homogenates (*upper lane*). Anti-actin Abs were used to normalize protein from lung homogenates (*lower lane*). Representative results are shown. Numbers shown above the bands are the mice identification numbers. Nine or more additional mice per group demonstrated similar results. *B*, Densitometry analysis of vitronectin expression in lung homogenates. Relative expression of vitronectin to actin in the lung homogenates of vitronectin$^{+/+}$ mice was analyzed using AlphaEase FC, densitometry measurement software. Each bar represents the average of five replicates ± SEM. ∗, $p < 0.05$. *C*, Western blotting for vitronectin in the lungs. Lungs were obtained from vitronectin$^{+/+}$ mice at 0, 1, 4, 8, or 24 h after LPS administration. Anti-mouse vitronectin IgG was used to detect vitronectin expression in the lung homogenates (*upper lane*). Anti-actin Abs were used to normalize protein from lung homogenates (*lower lane*). Representative results are shown. Numbers shown above the bands are the mice identification numbers. *D*, Immunohistochemistry for vitronectin in vitronectin$^{+/+}$ mice lungs obtained 24 h after intratracheal administration of PBS alone or PBS plus LPS (LPS). *Insets* in each panel are higher power images of the identical section. *E*, H&E staining of lungs obtained from vitronectin$^{+/+}$ or vitronectin$^{-/-}$ mice 24 h after intratracheal administration of PBS alone or PBS plus LPS (LPS).

Materials and Methods

Mice

Vitronectin-deficient mice with a targeted mutation of vitronectin (B6.129S2(D2)-*Vtn^{tm1Dgi}*/J, vitronectin$^{-/-}$), as well as age- and sex-matched control mice (C57BL/6J, vitronectin$^{+/+}$) on the same background, were purchased from The Jackson Laboratory. The genotypes of the vitronectin$^{-/-}$ and the vitronectin$^{+/+}$ control mice were confirmed by PCR analysis. Eight- to 10-wk-old male and female animals were used for experiments. The mice were kept on a 12-h light/dark cycle with free access to food and water. Animal protocols were reviewed and approved by the Institutional Animal Care and Use Committee of the University of Alabama at Birmingham.

Materials

Isoflurane was obtained from Minrad. LPS from *Escherichia coli* 0111:B4 was purchased from Sigma-Aldrich. RPMI 1640 medium with L-glutamine, sodium bicarbonate, and penicillin-streptomycin was obtained from Sigma-Aldrich, while FBS was purchased from Atlanta Biologicals. BSA, fraction V, was obtained from Fisher Scientific. Abs specific for phospho-p38 MAPK (Thr^{180}/Tyr^{182}), total p38 MAPK, phospho (Ser^{473})-Akt, and total Akt and IκB-α were purchased from Cell Signaling Technology. Rabbit anti-mouse vitronectin IgG was purchased from Oxford Biomedical Research. Anti-actin Abs were purchased from Sigma-Aldrich. Goat anti-rabbit IgG (H + L)-HRP conjugate was purchased from Bio-Rad. Custom mixture Abs and negative selection columns for neutrophil isolation were purchased from StemCell Technologies. Mouse vitronectin was obtained from Innovative Research. Recombinant murine KC was purchased from PeproTech. Collagen I was obtained from BD Biosciences.

In vivo acute lung injury model

ALI was induced by intratracheal administration of 1 mg/kg LPS in 50 μl of PBS. With this model, ALI, as characterized by neutrophil infiltration into the lung interstitium, development of interstitial edema, and increased proinflammatory cytokine production, occurs after injection of LPS, with the greatest accumulation of neutrophils into airways and histologic injury being present 24 h after LPS exposure (23–25). For this procedure, a blunt-end 22-gauge needle was passed through the mouth into the trachea in an isoflurane-anesthetized mouse and the LPS solution was deposited. There were no deaths associated with this model for intratracheal LPS exposure.

Harvest of lungs and bronchoalveolar lavage (BAL) fluid

Lungs were perfused with iced saline and harvested 24 h after LPS administration. BAL fluid samples were obtained from LPS-treated or control mice by cannulating the trachea with a 18-gauge Exel Safelet Cath (Excel International) and then lavaging the lungs three times with 1 ml of iced PBS. Total cell counts were measured in the BAL fluid with a hemocytometer (Hausser Scientific) and differential cell counts were determined after cytocentrifugation and staining with HEMA 3 (Fisher Scientific).

Serum preparation

Mouse whole blood was obtained from vitronectin$^{-/-}$ mice and centrifuged at room temperature. Serum was kept at −80°C until use.

Isolation of neutrophils

Mouse neutrophils were purified from bone marrow cell suspensions as described previously (26). Briefly, to obtain the bone marrow cell suspension, the femur and tibia of a mouse were flushed with 10 ml of RPMI 1640 medium/penicillin-streptomycin. The cells were passed through a 40-μm cell strainer (BD Biosciences) and then pelleted by centrifugation at 2000 rpm for 10 min. The cell pellets were resuspended in PBS and then incubated for 15 min, rotating at 4°C, with 20 μl of primary Abs specific for the cell surface markers F4/80, CD4, CD45R, CD5, and TER119. This custom mixture is specific for T and B cells, RBC, monocytes, and macrophages. Anti-biotin tetrameric Ab complexes (100 μl) were then added, and the cells were incubated for an additional 15 min at 4°C. Following this, 60 μl of colloidal magnetic dextran iron particles was added to the suspension and incubated for 15 min, rotating at 4°C. The entire cell suspension was then placed into a column surrounded by a magnet. The T cells, B cells, RBC, monocytes, and macrophages were captured in the column, allowing the neutrophils to pass through by negative selection. The cells were then pelleted and washed. Because of the differential density of platelets, there was no contamination with platelets in the final isolated neutrophil population. Neutrophil purity, as determined by HEMA 3-stained cytospin preparations, was >97%. Cell viability, as determined by trypan blue exclusion, was consistently >98%.

Preparation of lung homogenates and neutrophils for ELISA and Western blot analysis

Lung tissues were homogenized using a homogenizer (Glas-Col) in ice-cold lysis buffer (150 mM NaCl, 1% Triton X-100, 5 mM EDTA, 10 mM Tris, pH 7.4) supplemented with 1/100 protease inhibitor mixture (Sigma-Aldrich) and 1/100 phosphatase inhibitor mixtures I and II from AG Scientific. Homogenates were centrifuged at 14,000 × *g* for 30 min and supernatants were collected for ELISA and Western blot analysis. Bone marrow neutrophils (4×10^6/ml) were incubated in RPMI 1640 medium, 0.5% vitronectin$^{-/-}$ serum, penicillin-streptomycin, with or without 100 ng/ml LPS, in a humidified incubator (37°C, 5% CO_2, and 95% air). After LPS stimulation, culture medium was stored at −80°C. Cells were washed twice with PBS, resuspended in the same lysis buffer mentioned above, freeze-thawed once, sonicated, followed by centrifugation at 14,000 × *g* for 15 min. Supernatants were collected for Western blot analysis. The protein concentration of each sample was assayed using the DC protein assay kit (Bio-Rad) standardized to BSA according to the manufacturer's protocol.

Cytokine and chemokine ELISA and protein assays

Immunoreactive TNF-α, IL-1β, MIP-2, IL-6, and KC were quantified using commercially available DuoSet ELISA Development kits (R&D Systems) according to the manufacturer's instructions.

Myeloperoxidase (MPO) assay

MPO was measured using a modification of the method described by Goldblum et al. (27). In brief, lung tissue was homogenized using a Glas-Col homogenizer in 0.5 ml of 0.5% hexadecyltrimethylammonium bromide in 50 mM potassium phosphate buffer (pH 6.0). The homogenate was centrifuged at 14,000 × *g* for 30 min at 4°C and the supernatant was collected for assay of MPO activity as determined by measuring the H_2O_2-dependent oxidation of *o*-dianisidine solution (3,3′-dimethoxybenzidine dihydrochloride in potassium phosphate buffer, pH 6.0) at 450 nm. For determinations of MPO in BAL fluid samples, the MPO assay was performed using 10 μl of the BAL fluid, as described above.

Wet:dry lung weight ratios

All mice used for lung wet:weight ratios were of identical ages. Lungs were excised, rinsed briefly in PBS, blotted, and then weighed to obtain the "wet" weight. Lungs were then dried in an oven at 80°C for 7 days to obtain the "dry" weight.

Western blot analysis

For electrophoresis, 25 μg of total protein from lung homogenates and 15 μg of total protein from neutrophil lysates were loaded on 8% Tris-HCl SDS- PAGE. Protein was electrotransferred to a nitrocellulose membrane and then blocked with 5% nonfat dry milk in PBS with 0.1% Tween 20. After blocking, the membrane was incubated overnight at 4°C with specific primary Abs using a dilution of 1/1000–1/4000 followed by goat anti-rabbit IgG (H + L)-HRP conjugate secondary Ab at a dilution of 1/5000. After washing three times, bands were detected using SuperSignal West Pico Chemiluminescent Substrate (Pierce). The membranes were then stripped using ReBlot Plus Mild Ab Stripping Solution (Chemicon International) and reprobed with anti-actin Ab. Densitometry was performed using a chemiluminescence system (Bio-Rad) and analysis software

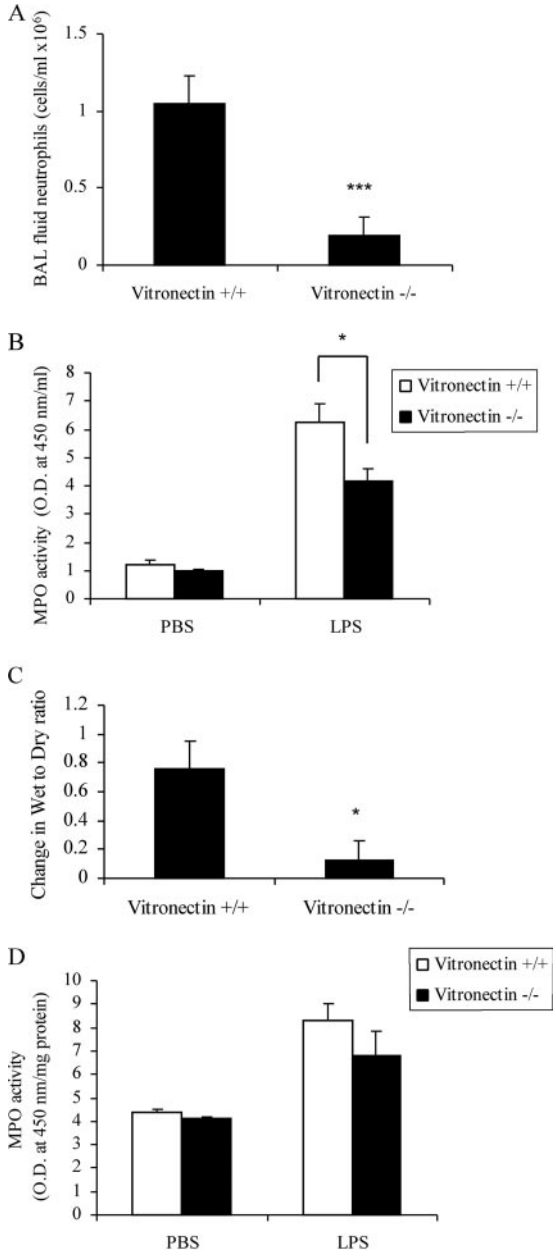

FIGURE 2. Vitronectin-deficient mice (vitronectin$^{-/-}$) are protected from LPS-induced ALI. *A*, Neutrophil counts in BAL fluid after intratracheal administration of LPS. BAL fluid was collected 24 h after LPS administration to vitronectin$^{-/-}$ or vitronectin$^{+/+}$ mice. Neutrophil counts in BAL fluid were determined by optical microscopy after cytocentrifugation and HEMA 3 staining. ***, $p < 0.005$ vs vitronectin$^{+/+}$ controls. *B*, MPO activity in BAL fluid after intratracheal administration of LPS. BAL fluid was collected at 24 h after LPS or PBS administration to vitronectin$^{+/+}$ mice (□) or vitronectin$^{-/-}$ mice (■). *, $p < 0.05$. *C*, Wet:dry lung weight ratios at 24 h after intratracheal administration of LPS to vitronectin$^{+/+}$ or vitronectin$^{-/-}$ mice. The increase in wet:dry ratio for each LPS-treated animal was calculated by subtracting the mean value for control, unmanipulated mice of the same strain. *, $p < 0.05$ vs vitronectin$^{+/+}$ control. *D*, Lung MPO levels measured 24 h after intratracheal administration of LPS or PBS. Results from vitronectin$^{+/+}$ (□) and vitronectin$^{-/-}$ mice (■) are shown. Each experimental group consisted of 3–10 mice. Means ± SEM are shown. One (*A*) or two (*B* and *D*) additional experiments with separate groups of mice provided similar results.

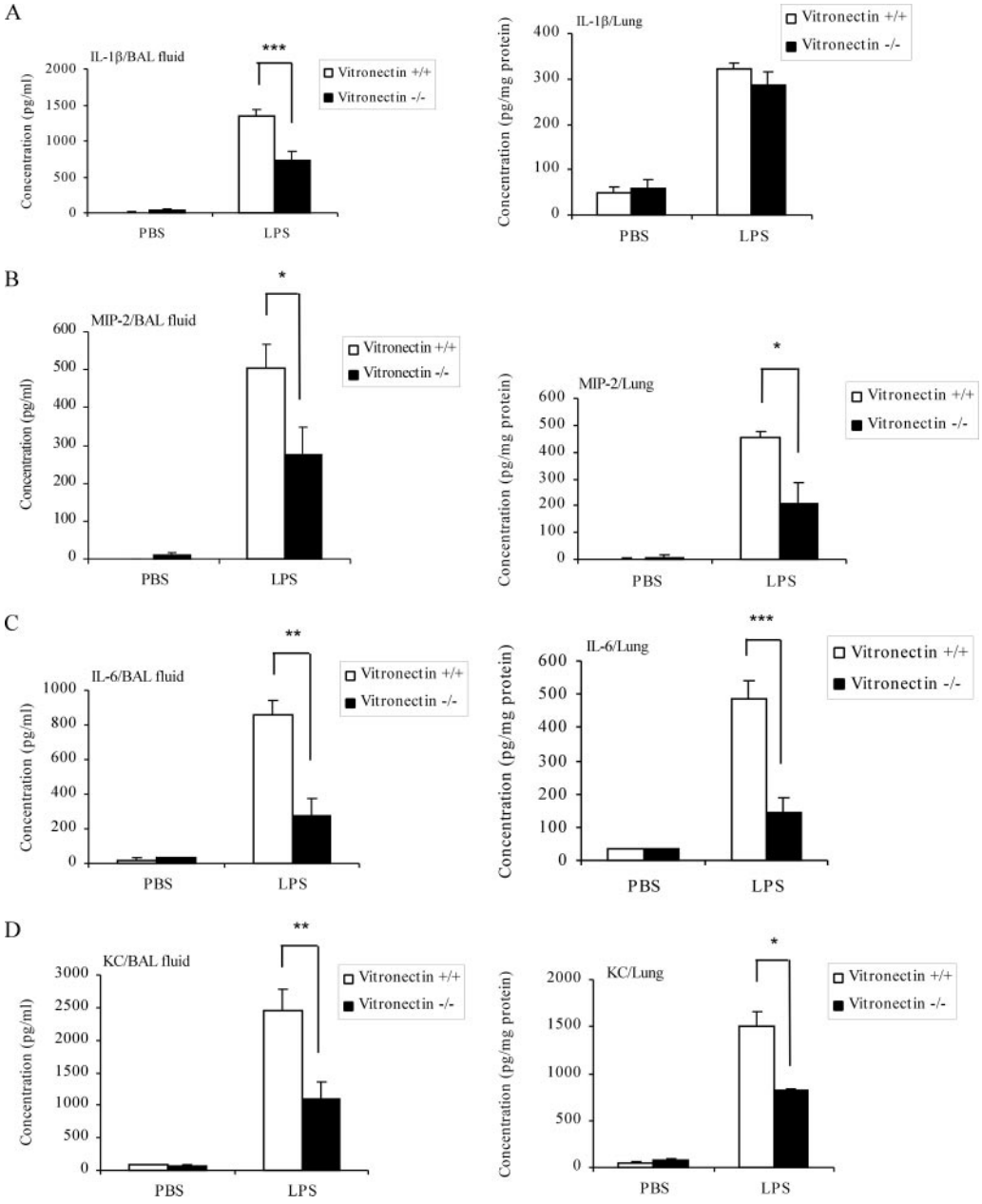

FIGURE 3. Vitronectin $^{-/-}$ mice are protected from LPS-induced ALI. *A–D*, BAL fluid (*left panel*) and pulmonary homogenate concentrations (*right panel*) of IL-1β (*A*), MIP-2 (*B*), IL-6 (*C*), and KC (*D*). BAL fluid and lung homogenates were collected at 24 h after intratracheal LPS or PBS administration to vitronectin$^{-/-}$ (■) or vitronectin$^{+/+}$ (□) mice. Results for lung homogenates are shown as picograms of cytokine per milligram of total lung protein. Each experimental group consisted of 3–10 mice. Means ± SEM are shown. *, $p < 0.05$; **, $p < 0.01$; and ***, $p < 0.005$. Two additional experiments with separate groups of mice demonstrated similar results.

AlphaEase FC (Alpha Innotech) to determine relative expression of specific protein to actin.

Migration assay

For the preincubation group, 1×10^5 purified neutrophils were incubated with or without 50 nM mouse vitronectin in 100 μl of RPMI 1640 medium in a humidified incubator (37°C, 5% CO_2, and 95% air) for 15 min. A total of 1×10^5 purified neutrophils was added to the upper compartment of a MultiScreen Migration Invasion and Chemotaxis (MIC) plate (3-μm pore, 96-well; Millipore), where Transwell membranes were coated without or with 5 μg/ml collagen I or mouse vitronectin and bathed in RPMI 1640 medium containing 0.5% vitronectin$^{-/-}$ serum. Recombinant murine KC was added to the lower compartment at a concentration of 100 ng/ml in 150 μl of RPMI 1640 medium containing 0.5% FBS. The chemotaxis apparatus was placed in a humidified incubator (37°C, 5% CO_2, and 95% air) for 30 min. The upper face of the MultiScreen MIC plate filter was wiped with a cotton swab to remove remaining neutrophils and then the lower face of the MultiScreen MIC plate filter was fixed and stained using HEMA 3. The numbers of neutrophils that migrated through the MultiScreen MIC plate filter were counted under a light microscope.

EMSA

Nuclear extracts were prepared and assayed by EMSA as previously described (28–32). For analysis of NF-κB, the κB DNA sequence of the Ig gene was used. Synthetic double-stranded sequences (with enhancer motifs underlined) were filled in and labeled with [γ-^{32}P]dATP (GE Healthcare) using Sequenase DNA polymerase as follows: κB sequence, 5′-GCCATGGGGGGATCCCCGAAGTCC-3′ (Geneka Biotechnology).

Histopathology

Mouse lungs were inflation fixed with 10% formaldehyde at 20 cm H_2O pressure and embedded in paraffin for sectioning at 6-μm thickness. The sections were stained with H&E. Immunoperoxidase staining was performed on the paraffin-embedded sections of mouse lung as described previously (33, 34).

Statistical analysis

For each experimental condition, the entire group of animals was prepared and studied at the same time. Data are presented as mean ± SD (in vitro experiments) or ± SEM (in vivo experiments) for each experimental group. Student's *t* test was used for comparisons between the two groups. A value of $p < 0.05$ was considered significant.

Results

LPS exposure induces vitronectin expression in the lungs

As an initial approach to investigate the role of vitronectin in ALI, we analyzed pulmonary levels of vitronectin following intratracheal administration of LPS. As shown in Fig. 1, *A–C*, vitronectin concentrations in the lungs were significantly increased ($p < 0.01$) 24 h after exposure to LPS.

Histologic sections from control, unmanipulated mice or mice given PBS alone intratracheally 24 h previously showed minimal staining for vitronectin, with only occasional alveolar macrophages being vitronectin positive (Fig. 1*D*). In contrast, 24 h after LPS administration, there was diffuse reactivity of the lungs for vitronectin, with alveolar macrophages, epithelial cells, and the intra-alveolar space all being intensively positive (Fig. 1*D*).

Vitronectin$^{-/-}$ mice are protected against LPS-induced ALI

To explore the importance of vitronectin in the development of ALI, vitronectin-deficient (vitronectin$^{-/-}$) and control vitronectin$^{+/+}$ mice were exposed to intratracheal LPS. As shown in Fig. 1*E*, 24 h after LPS exposure, the lungs of vitronectin$^{+/+}$ mice showed accumulation of inflammatory cells, primarily neutrophils, as well as increased interstitial edema and leakage of RBCs into the alveolar space. In contrast, there was only minimally increased neutrophil accumulation in the lungs of the LPS-exposed vitronectin$^{-/-}$ mice.

Significantly fewer neutrophils were found in BAL fluid obtained from vitronectin$^{-/-}$ mice 24 h after LPS administration as compared with neutrophil numbers in BAL fluid from vitronectin$^{+/+}$ mice (Fig. 2*A*). MPO levels in BAL fluid and lungs from vitronectin$^{-/-}$ mice were also significantly lower than those found in vitronectin$^{+/+}$ mice (Fig. 2, *B* and *D*). Similarly, lung edema, as determined by the increase in the wet:dry lung weight ratio after LPS administration, was significantly less in the vitronectin$^{-/-}$ mice compared with control vitronectin$^{+/+}$ animals (Fig. 2*C*).

The absence of vitronectin was associated with significantly lower levels of proinflammatory cytokines in BAL fluid and lung homogenates after LPS administration. In particular, lung and BAL fluid concentrations of IL-1β, MIP-2, KC, and IL-6 were significantly lower in vitronectin$^{-/-}$ mice as compared with those present in vitronectin$^{+/+}$ controls (Fig. 3).

Vitronectin contributes to neutrophil chemotaxis, but not cytokine production, in LPS-exposed neutrophils

The accumulation of neutrophils activated to produce proinflammatory mediators, including cytokines and chemokines, plays a central role in determining the severity of pulmonary injury after LPS exposure. To explore potential mechanisms that may contribute to the reduction in pulmonary inflammation found in vitronectin$^{-/-}$ mice, we examined chemotaxis and production of proinflammatory cytokines by vitronectin$^{-/-}$ and control vitronectin$^{+/+}$ neutrophils. Vitronectin$^{-/-}$ neutrophils consistently produced more TNF-α, MIP-2, and IL-1β after LPS exposure than did those from vitronectin$^{+/+}$ mice (Fig. 4).

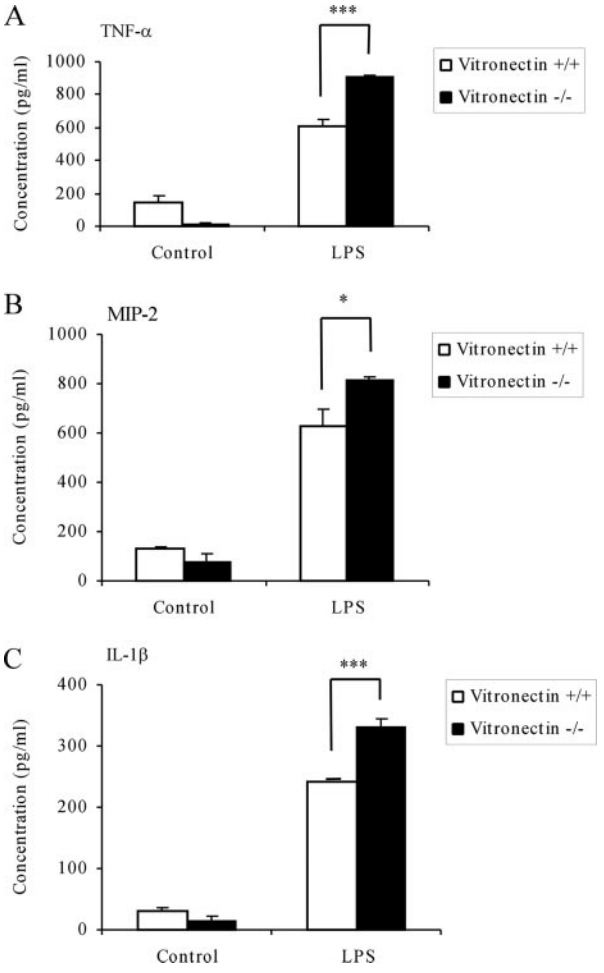

FIGURE 4. Vitronectin$^{-/-}$ *n*eutrophils produce greater amounts of proinflammatory cytokines after LPS exposure than do those from vitronectin$^{+/+}$ mice. Neutrophils from vitronectin$^{-/-}$ (■) or vitronectin$^{+/+}$ (□) mice were incubated without (Control) or with 100 ng/ml LPS for 4 h. TNF-α (*A*), MIP-2 (*B*), and IL-1β (*C*) were measured in the culture supernatants by ELISA. Means ± SD are shown. *, $p < 0.05$ and ***, $p < 0.005$. A representative experiment using neutrophils pooled from two vitronectin$^{-/-}$ or vitronectin$^{+/+}$ mice and performed in triplicate is shown. Five additional experiments with separate groups of mice demonstrated similar results.

Because KC is a potent chemoattractant that is increased in acute lung injury (Fig. 3*D*) and has been shown to contribute to pulmonary neutrophil accumulation associated with LPS-induced lung injury (35), we examined KC-induced chemotaxis of vitronectin$^{-/-}$ and vitronectin$^{+/+}$ neutrophils. As shown in Fig. 5*A*, vitronectin$^{+/+}$ neutrophils demonstrated significantly greater accumulation across a KC-induced gradient than did vitronectin$^{-/-}$ neutrophils.

To further investigate the role of vitronectin on KC-induced chemotaxis, we used vitronectin-coated membranes as well as exposure of neutrophils to vitronectin-containing medium. When vitronectin$^{+/+}$ neutrophils were incubated on vitronectin-coated plates, neutrophil migration to KC was enhanced as compared with that found with neutrophils incubated on uncoated plates (Fig. 5*A*). Preincubation of vitronectin$^{+/+}$ neutrophils with recombinant vitronectin protein for 15 min also resulted in significantly increased KC-induced chemotaxis as compared with that found without vitronectin exposure (Fig. 5*B*).

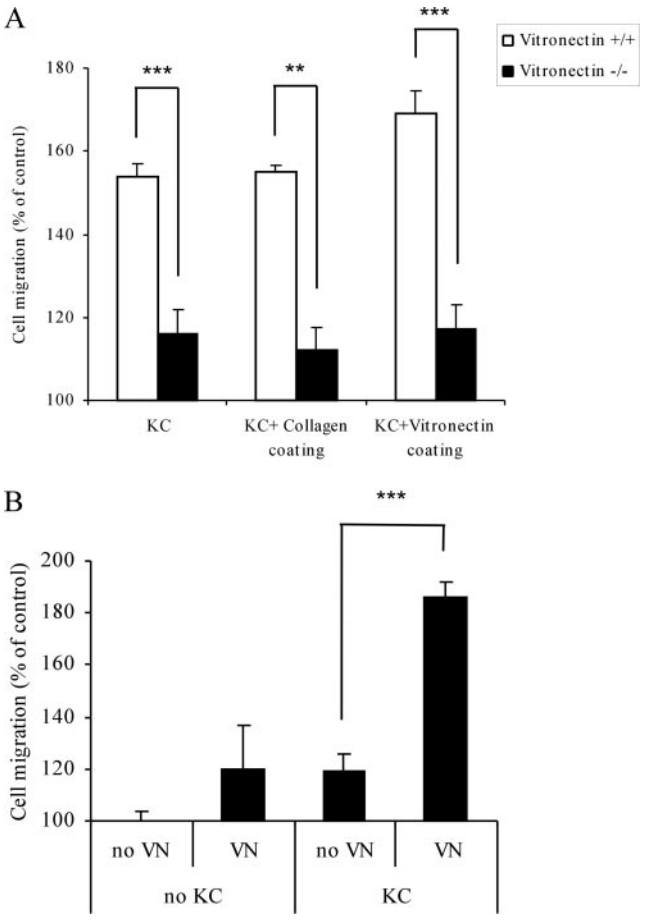

FIGURE 5. Exposure to increased extracellular concentrations of vitronectin (VN) enhances neutrophil chemotaxis. *A*, Neutrophils from vitronectin$^{-/-}$ (■) or vitronectin$^{+/+}$ (□) mice were incubated in the upper compartment of 96-well MultiScreen MIC plates, with or without addition of 100 ng/ml recombinant murine KC to the lower compartment of the same plate, with Transwell membranes either coated or not with 5 μg/ml collagen I or mouse vitronectin. The cells that migrated through the Transwell membranes after a 30-min incubation were then counted. Results are expressed as a percentage of neutrophils crossing the membrane under untreated conditions (control). *B*, Neutrophils from vitronectin$^{+/+}$ mice were preincubated without or with 50 nM mouse vitronectin for 15 min and then chemotaxis to KC was determined. Means ± SD are shown. **, $p < 0.01$ and ***, $p < 0.005$. A representative experiment using neutrophils pooled from three vitronectin$^{-/-}$ or vitronectin$^{+/+}$ mice and performed in triplicate is shown. Two additional experiments with separate groups of mice demonstrated similar results.

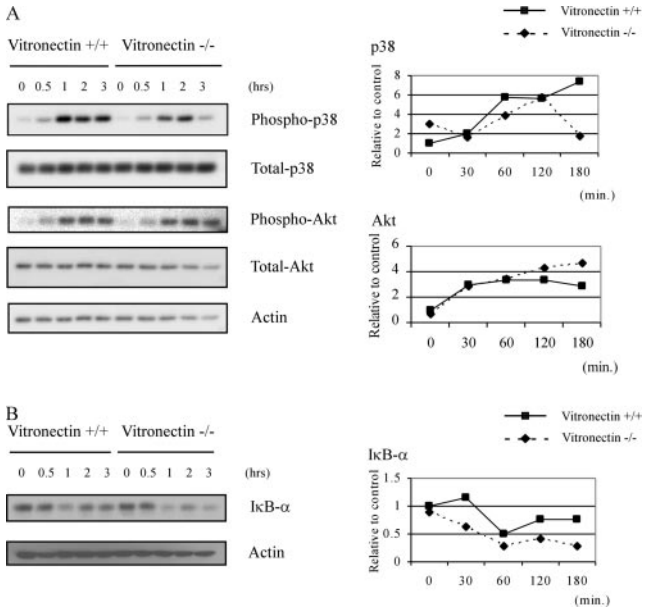

FIGURE 6. LPS-induced alterations in IκB-α levels and phosphorylation of the p38 MAPK and Akt in vitronectin$^{-/-}$ and vitronectin$^{+/+}$ neutrophils. After incubation with 100 ng/ml LPS, cell extracts were prepared and Western blots were performed to detect phosphorylated forms of p38 MAPK (Phospho-p38, *A*, *left panel*), total p38 MAPK (Total-p38, *A*, *left panel*), as well as phosphorylated Akt (Phospho-Akt, *A*, *left panel*), total Akt (Total-Akt, *A*, *left panel*), and total IκB-α (*B*, *left panel*). Densitometry determinations are presented of the relative expression of phosphorylated forms of p38 MAPK to total p38 MAPK (p38, *A*, *right panel*), phosphorylated Akt to total Akt (Akt, *A*, *right panel*), and total IκB-α to actin (IκB-α, *B*, *right panel*) in the cell extracts of vitronectin$^{-/-}$ (dotted line) or vitronectin$^{+/+}$ (straight line) mice. A representative experiment is shown using neutrophils pooled from three vitronectin$^{-/-}$ or vitronectin$^{+/+}$ mice. Three additional experiments with separate groups of mice provided similar results.

Effects of vitronectin on LPS-induced kinase and NF-κB activation

TLR4 engagement results in activation of multiple kinases involved in proinflammatory cytokine expression and NF-κB activation (36, 37). Pathways leading to phosphorylation of the p38 MAPK and Akt appear to be particularly important in LPS-induced neutrophil activation (26, 32, 38).

To examine the effects of vitronectin on kinase activation after LPS stimulation, we incubated vitronectin$^{+/+}$ or vitronectin$^{-/-}$ neutrophils with LPS and then determined the levels of the active, phosphorylated forms of p38 MAPK and Akt. Similar levels of Akt phosphorylation were found in both vitronectin$^{+/+}$ and vitronectin$^{-/-}$ neutrophils within 30 min of exposure to LPS and continued to be present over the 3-h period examined (Fig. 6*A*). In contrast, p38 phosphorylation was persistently present during the 3 h after LPS exposure in vitronectin$^{+/+}$ neutrophils, but had diminished at the 3-h time point in vitronectin$^{-/-}$ neutrophils.

Levels of IκB-α in vitronectin$^{+/+}$ neutrophils were maximally reduced within 1 h after exposure to LPS and then slowly increased at later time points. In contrast, in vitronectin$^{-/-}$ neutrophils, decreased IκB-α levels continued to be present over the 3-h period examined (Fig. 6*B*). Nuclear concentrations of NF-κB were increased in both vitronectin$^{+/+}$ and vitronectin$^{-/-}$ neutrophils over the 3 h after exposure to LPS, with greater nuclear levels of NF-κB being present in the vitronectin$^{-/-}$ neutrophils, particularly at later time points (Fig. 7).

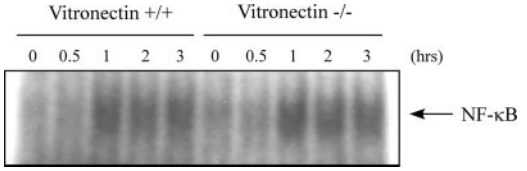

FIGURE 7. Nuclear translocation of NF-κB in vitronectin$^{-/-}$ and vitronectin$^{+/+}$ neutrophils after LPS exposure. After incubation with 100 ng/ml LPS, nuclear extracts were prepared and EMSA was performed to detect nuclear NF-κB accumulation. Representative EMSA gels are presented. Two additional experiments with separate groups of mice provided similar results.

Discussion

Although increased concentrations of vitronectin have been reported in the lungs of patients with sepsis (21, 22), there has been little information to suggest that vitronectin was directly involved in the development of acute lung injury. In the present experiments, we found that vitronectin-deficient mice were protected from LPS-induced lung injury, with decreased pulmonary interstitial edema, neutrophil accumulation, and proinflammatory cytokine production as compared with wild-type control mice. The diminished severity of lung injury in the vitronectin knockout mice was not due to inhibition of neutrophil proinflammatory responses, because the levels of cytokine production by LPS-stimulated vitronectin$^{-/-}$ neutrophils were consistently higher than those generated by vitronectin$^{+/+}$ neutrophils. In contrast, chemotaxis of vitronectin$^{-/-}$ neutrophils to KC, a CXC chemokine previously demonstrated to play an important role in pulmonary neutrophil accumulation in experimental models of pneumonia or LPS exposure (35), were significantly decreased as compared with vitronectin$^{+/+}$ neutrophils. Taken together, these results would indicate that the primary role by which vitronectin participates in enhancing acute lung injury is through its effects on neutrophil chemotaxis.

Even though vitronectin also appears to have down-regulating properties on neutrophil activation to produce proinflammatory cytokines, as shown by the greater production of proinflammatory cytokines by vitronectin$^{-/-}$ neutrophils, these effects seem to be less important in the pathogenesis of acute lung injury than is the ability of vitronectin to mediate neutrophil accumulation in the lungs. Such findings are consistent with the fact that the production of proinflammatory cytokines by individual neutrophils is relatively modest, especially as compared with amounts produced by macrophages, and that the central role of neutrophils in contributing to acute lung injury relates more to the extremely large numbers of neutrophils that accumulate in the tissues during inflammatory processes rather than the production of proinflammatory mediators by individual neutrophils (4, 39, 40).

In the present experiments, the amounts of vitronectin present in the lungs were increased after administration of LPS, consistent with previously reported results in humans (21, 22). Alveolar macrophages were the primary cell populations staining for vitronectin in LPS- exposed lungs, similar to findings in lungs from patients with severe sepsis (21, 22). Previous studies have shown that vitronectin participates in chemotaxis of neutrophils and other cellular populations, both through interactions with integrins, such as $\alpha_V\beta_3$, and other receptors, such as uPAR (20). We found that chemotaxis of vitronectin$^{+/+}$ neutrophils across vitronectin-coated membranes was enhanced, suggesting that alterations in extracellular vitronectin concentrations may modulate neutrophil migration across chemotactic gradients, such as those that exist in the LPS-exposed lung (41–43). It is therefore likely that the increased pulmonary concentrations of vitronectin present during sepsis or after LPS administration directly contribute to the accumulation of neutrophils in the lungs and airways through enhancing chemotaxis toward chemokines and other proinflammatory mediators released in these settings. Of note, KC, the CXC chemokine used in the present in vitro chemotaxis assays, is not only significantly elevated in the lungs after LPS administration, but also has been demonstrated to play an important role in pulmonary neutrophil accumulation in models of acute lung injury (35, 41–43). Because the presence of activated neutrophils in the lungs is an important contributor to acute lung injury (4), mechanisms that diminish neutrophil migration and accumulation, such as reduction of pulmonary vitronectin concentrations, would be expected to result in decreased severity of lung injury.

Neutrophils from vitronectin-deficient mice demonstrated decreased chemotaxis as compared with neutrophils from wild-type mice. Phosphorylation of the p38 MAPK after LPS exposure was less persistent in vitronectin$^{-/-}$ neutrophils as compared with that found in neutrophils from vitronectin$^{+/+}$ mice. Since p38 MAPK plays a central role in neutrophil chemotaxis (43, 44), the diminished activation of this kinase is likely to contribute to the reduced accumulation of neutrophils into the lungs of vitronectin$^{-/-}$ mice found in these studies.

Despite the alterations in chemotaxis, vitronectin$^{-/-}$ neutrophils have a greater proinflammatory phenotype as compared with vitronectin$^{+/+}$ neutrophils after culture with LPS, with increased release of proinflammatory cytokines, prolonged degradation of IκB-α, and slightly enhanced nuclear translocation of NF-κB in the vitronectin$^{-/-}$ neutrophils. These differences between vitronectin$^{-/-}$ and vitronectin$^{+/+}$ neutrophils in function and proinflammatory response may reflect the presence and actions of vitronectin on the neutrophil membrane. Vitronectin is present in high concentrations in serum (45) and neutrophils from wild-type mice demonstrate intense surface staining for vitronectin, probably as a result of contact with circulating vitronectin. In addition to its ability to enhance cellular migration (46), vitronectin has been demonstrated to diminish cellular activation through its interactions with integrins, including $\alpha_V\beta_3$ and $\alpha_M\beta_2$, as well as other receptors, such as CD47 (15, 47). Therefore, since there is no circulating vitronectin in vitronectin$^{-/-}$ mice, neutrophils from such animals will lack surface vitronectin and would be expected to have both enhanced proinflammatory responses as well as diminished chemotaxis, as found in these studies.

Even though serum levels of vitronectin are high under normal conditions, with concentrations approaching 400 μg/ml (45), the present studies suggest that the enhanced pulmonary concentrations of vitronectin in the setting of sepsis may contribute to neutrophil accumulation in the lungs and localized inflammatory injury. In chemotaxis assays, we found that increased local concentrations of vitronectin, produced by coating membranes with vitronectin, resulted in greater neutrophil migration even though the cells had already been exposed to serum containing high levels of vitronectin. Such results suggest that therapies able to reduce pulmonary concentrations of vitronectin or block interaction of vitronectin with integrins or receptors, such as uPAR, that participate in neutrophil chemotaxis may have clinical utility in diminishing the severity of acute lung injury.

Disclosures

The authors have no financial conflict of interest.

References

1. Rubenfeld, G. D., E. Caldwell, E. Peabody, J. Weaver, D. P. Martin, M. Neff, E. J. Stern, and L. D. Hudson. 2005. Incidence and outcomes of acute lung injury. *N. Engl. J. Med.* 353: 1685–1693.
2. Matthay, M. A., G. A. Zimmerman, C. Esmon, J. Bhattacharya, B. Coller, C. M. Doerschuk, J. Floros, M. A. Gimbrone, Jr., E. Hoffman, R. D. Hubmayr, et al. Future research directions in acute lung injury: summary of a National Heart, Lung, and Blood Institute working group. *Am. J. Respir. Crit. Care Med.* 167: 1027–1035.
3. Chignard, M., and V. Balloy. 2000. Neutrophil recruitment and increased permeability during acute lung injury induced by lipopolysaccharide. *Am. J. Physiol.* 279: L1083–L1090.
4. Abraham, E., A. Carmody, R. Shenkar, and J. Arcaroli. 2000. Neutrophils as early immunologic effectors in hemorrhage- or endotoxemia-induced acute lung injury. *Am. J. Physiol.* 279: L1137–L1145.
5. Azoulay, E., M. Darmon, C. Delclaux, F. Fieux, C. Bornstain, D. Moreau, H. Attalah, J. R. Le Gall, and B. Schlemmer. 2002. Deterioration of previous acute lung injury during neutropenia recovery. *Crit. Care Med.* 30: 781–786.
6. Idell, S. 2002. Endothelium and disordered fibrin turnover in the injured lung: newly recognized pathways. *Crit. Care Med.* 30: S274–S280.

7. Shetty, S., K. Bdeir, D. B. Cines, and S. Idell. 2003. Induction of plasminogen activator inhibitor-1 by urokinase in lung epithelial cells. *J. Biol. Chem.* 278: 18124–18131.
8. Quax, P. H., C. M. van den Hoogen, J. Verheijen, T. Padro, R. Zeheb, T. D. Gelehrter, T. J. van Berkel, K. J., and J. J. Emeis. 1990. Endotoxin induction of plasminogen activator and plasminogen activator inhibitor type 1 mRNA in rat tissues in vivo. *J. Biol. Chem.* 265: 15560–15563.
9. Abraham, E., M. R. Gyetko, K. Kuhn, J. Arcaroli, D. Strassheim, J. S. Park, S. Shetty, and S. Idell. 2003. Urokinase-type plasminogen activator potentiates lipopolysaccharide-induced neutrophil activation. *J. Immunol.* 170: 5644–5651.
10. Kwak, S. H., X. Q. Wang, Q. He, W. F. Fang, S. Mitra, K. Bdeir, V. A. Ploplis, Z. Xu, S. Idell, D. Cines, and E. Abraham. 2006. Plasminogen activator inhibitor-1 potentiates LPS-induced neutrophil activation through a JNK-mediated pathway. *Thromb. Haemost.* 95: 829–835.
11. Prabhakaran, P., L. B. Ware, K. E. White, M. T. Cross, M. A. Matthay, and M. A. Olman. 2003. Elevated levels of plasminogen activator inhibitor-1 in pulmonary edema fluid are associated with mortality in acute lung injury. *Am. J. Physiol.* 285: L20–L28.
12. Wang, X. Q., K. Bdeir, S. Yarovoi, D. B. Cines, W. Fang, and E. Abraham. 2006. Involvement of the urokinase kringle domain in lipopolysaccharide-induced acute lung injury. *J. Immunol.* 177: 5550–5557.
13. Kwak, S. H., S. Mitra, K. Bdeir, D. Strassheim, J. S. Park, J. Y. Kim, S. Idell, D. Cines, and E. Abraham. 2005. The kringle domain of urokinase-type plasminogen activator potentiates LPS-induced neutrophil activation through interaction with $\alpha_V\beta_3$ integrins. *J. Leukocyte Biol.* 78: 937–945.
14. Blasi, F., and P. Carmeliet. 2002. uPAR: a versatile signalling orchestrator. *Nat. Rev. Mol. Cell Biol.* 3: 932–943.
15. Reuning, U., V. Magdolen, S. Hapke, and M. Schmitt. 2003. Molecular and functional interdependence of the urokinase-type plasminogen activator system with integrins. *Biol. Chem.* 384: 1119–1131.
16. Preissner, K. T., and D. Jenne. 1991. Vitronectin: a new molecular connection in haemostasis. *Thromb. Haemost.* 66: 189–194.
17. Preissner, K. T., and D. Jenne. 1991. Structure of vitronectin and its biological role in haemostasis. *Thromb. Haemost.* 66: 123–132.
18. Preissner, K. T. 1989. The role of vitronectin as multifunctional regulator in the hemostatic and immune systems. *Blut* 59: 419–431.
19. Tomasini, B. R., and D. F. Mosher. 1991. *Vitronectin Prog. Hemost. Thromb.* 10: 269–305.
20. Kanse, S. M., R. L. Matz, K. T. Preissner, and K. Peter. 2004. Promotion of leukocyte adhesion by a novel interaction between vitronectin and the β_2 integrin Mac-1 ($\alpha_M\beta_2$, CD11b/CD18). *Arterioscler. Thromb. Vasc. Biol.* 24: 2251–2256.
21. Singh, B., K. S. Janardhan, and R. Kanthan. 2005. Expression of angiostatin, integrin $\alpha_v\beta_3$, and vitronectin in human lungs in sepsis. *Exp. Lung Res.* 31: 771–782.
22. Simon, D. I., N. K. Rao, H. Xu, Y. Wei, O. Majdic, E. Ronne, L. Kobzik, and H. A. Chapman. 1996. Mac-1 (CD11b/CD18) and the urokinase receptor (CD87) form a functional unit on monocytic cells. *Blood* 88: 3185–3194.
23. Asti, C., V. Ruggieri, S. Porzio, R. Chiusaroli, G. Melillo, and G. F. Caselli. 2000. Lipopolysaccharide-induced lung injury in mice: I. Concomitant evaluation of inflammatory cells and haemorrhagic lung damage. *Pulm. Pharmacol. Ther.* 13: 61–69.
24. Abraham, E., J. Arcaroli, A. Carmody, H. Wang, and K. J. Tracey. 2000. HMG-1 as a mediator of acute lung inflammation. *J. Immunol.* 165: 2950–2954.
25. Rowe, S. J., L. Allen, V. C. Ridger, P. G. Hellewell, and M. K. Whyte. 2002. Caspase-1-deficient mice have delayed neutrophil apoptosis and a prolonged inflammatory response to lipopolysaccharide-induced acute lung injury. *J. Immunol.* 169: 6401–6407.
26. Yum, H. K., J. Arcaroli, J. Kupfner, R. Shenkar, J. M. Penninger, T. Sasaki, K. Y. Yang, J. S. Park, and E. Abraham. 2001. Involvement of phosphoinositide 3-kinases in neutrophil activation and the development of acute lung injury. *J. Immunol.* 167: 6601–6608.
27. Goldblum, S. E., K. M. Wu, and M. Jay. 1985. Lung myeloperoxidase as a measure of pulmonary leukostasis in rabbits. *J. Appl. Physiol.* 59: 1978–1985.
28. Dignam, J. D., P. L. Martin, B. S. Shastry, and R. G. Roeder. 1983. Eukaryotic gene transcription with purified components. *Methods Enzymol.* 101: 582–598.
29. Dignam, J. D., R. M. Lebovitz, and R. G. Roeder. 1983. Accurate transcription initiation by RNA polymerase II in a soluble extract from isolated mammalian nuclei. *Nucleic Acids Res.* 11: 1475–1489.
30. Baeuerle, P. A. 1998. IκB-NF-κB structures: at the interface of inflammation control. *Cell* 95: 729–731.
31. Shenkar, R., M. D. Schwartz, L. S. Terada, J. E. Repine, J. McCord, and E. Abraham. 1996. Hemorrhage activates NF-κB in murine lung mononuclear cells in vivo. *Am. J. Physiol.* 270: L729–L735.
32. Yang, K. Y., J. J. Arcaroli, and E. Abraham. 2003. Early alterations in neutrophil activation are associated with outcome in acute lung injury. *Am. J. Respir. Crit. Care Med.* 167: 1567–1574.
33. Hamid, A. A., M. Mandai, I. Konishi, K. Nanbu, Y. Tsuruta, T. Kusakari, M. Kariya, M. Kita, and S. Fujii. 2002. Cyclical change of hMSH2 protein expression in normal endometrium during the menstrual cycle and its overexpression in endometrial hyperplasia and sporadic endometrial carcinoma. *Cancer* 94: 997–1005.
34. Yamamoto, S., I. Konishi, Y. Tsuruta, K. Nanbu, M. Mandai, H. Kuroda, K. Matsushita, A. A. Hamid, Y. Yura, and T. Mori. 1997. Expression of vascular endothelial growth factor (VEGF) during folliculogenesis and corpus luteum formation in the human ovary. *Gynecol. Endocrinol.* 11: 371–381.
35. Frevert, C. W., S. Huang, H. Danaee, J. D. Paulauskis, and L. Kobzik. 1995. Functional characterization of the rat chemokine KC and its importance in neutrophil recruitment in a rat model of pulmonary inflammation. *J. Immunol.* 154: 335–344.
36. Chen, L. F., and W. C. Greene. 2004. Shaping the nuclear action of NF-κB. *Nat. Rev. Mol. Cell Biol.* 5: 392–401.
37. Abraham, E., J. A. Nick, T. Azam, S. H. Kim, J. P. Mira, D. Svetkauskaite, Q. He, M. Zamora, J. Murphy, J. S. Park, K. Overdier, and C. A. Dinarello. 2006. Peripheral blood neutrophil activation patterns are associated with pulmonary inflammatory responses to lipopolysaccharide in humans. *J. Immunol.* 176: 7753–7760.
38. Arcaroli, J., K. Y. Yang, H. K. Yum, J. Kupfner, T. M. Pitts, J. S. Park, D. Strassheim, and E. Abraham. 2002. Effects of catecholamines on kinase activation in lung neutrophils after hemorrhage or endotoxemia. *J. Leukocyte Biol.* 72: 571–579.
39. Abraham, E. 2003. Neutrophils and acute lung injury. *Crit. Care Med.* 31: S195–S199.
40. Parsey, M. V., R. M. Tuder, and E. Abraham. 1998. Neutrophils are major contributors to intraparenchymal lung IL-1β expression after hemorrhage and endotoxemia. *J. Immunol.* 160: 1007–1013.
41. Arndt, P. G., S. K. Young, and G. S. Worthen. 2005. Regulation of lipopolysaccharide-induced lung inflammation by plasminogen activator inhibitor-1 through a JNK-mediated pathway. *J. Immunol.* 175: 4049–4059.
42. Lomas-Neira, J., C. S. Chung, M. Perl, S. Gregory, W. Biffl, and A. Ayala. 2006. Role of alveolar macrophage and migrating neutrophils in hemorrhage-induced priming for ALI subsequent to septic challenge. *Am. J. Physiol.* 290: L51–L58.
43. Nick, J. A., S. K. Young, P. G. Arndt, J. G. Lieber, B. T. Suratt, K. R. Poch, N. J. Avdi, K. C. Malcolm, C. Taube, P. M. Henson, and G. S. Worthen. 2002. Selective suppression of neutrophil accumulation in ongoing pulmonary inflammation by systemic inhibition of p38 mitogen-activated protein kinase. *J. Immunol.* 169: 5260–5269.
44. Cara, D. C., J. Kaur, M. Forster, D. M. McCafferty, and P. Kubes. 2001. Role of p38 mitogen-activated protein kinase in chemokine-induced emigration and chemotaxis in vivo. *J. Immunol.* 167: 6552–6558.
45. Boyd, N. A., A. R. Bradwell, and R. A. Thompson. 1993. Quantitation of vitronectin in serum: evaluation of its usefulness in routine clinical practice. *J. Clin. Pathol.* 46: 1042–1045.
46. Preissner, K. T., and D. Seiffert. 1998. Role of vitronectin and its receptors in haemostasis and vascular remodeling. *Thromb. Res.* 89: 1–21.
47. Hermann, P., M. Armant, E. Brown, M. Rubio, H. Ishihara, D. Ulrich, R. G. Caspary, F. P. Lindberg, R. Armitage, C. Maliszewski, G. Delespesse, and M. Sarfati. 1999. The vitronectin receptor and its associated CD47 molecule mediates proinflammatory cytokine synthesis in human monocytes by interaction with soluble CD23. *J. Cell Biol.* 144: 767–775.